Journal of Electronics, Electromedical Engineering, and Medical Informatics
Homepage: jeeemi.org; Vol. 8, No. 2, April 2026, pp: 517-536 e-ISSN: 2656-8632

RESEARCH ARTICLE OPEN ACCESS

Design and Statistical Evaluation of an AI-Enabled IoT-Based Non-Invasive Biosensing System for Diabetes Risk Screening

Prachi Kamble[1], Lakshmappa Ragha[1], and Yogesh Pingle[2]

[1] Department of Electronics Engineering, Terna Engineering College, University of Mumbai, Maharashtra, India
[2] Department of Computer Science & Engineering (Data Science), Vidyavardhini's College of Engineering & Technology, University of Mumbai, Maharashtra, India

Corresponding author: Prachi Kamble (e-mail: prachikamble@ternaengg.ac.in), **Author(s) Email**: Lakshmappa Ragha (e-mail: lkragha@gmail.com, Yogesh Pingle (e-mail: yogesh.pingle@vcet.edu.in)

Abstract **Early identification of diabetes risk remains a significant challenge due to the invasive nature, recurring cost, and limited accessibility of conventional biochemical diagnostic tests. These limitations restrict continuous monitoring and hinder large-scale population screening, particularly in remote and resource-limited settings. The aim of this study is to design and statistically evaluate an AI-enabled IoT-based non-invasive biosensing system for diabetes risk screening, focusing on system-level engineering design, data integration, and performance validation rather than clinical diagnosis. In this study, the term "non-invasive" refers exclusively to externally measurable surface-level physiological and breath-based signals that do not require skin penetration, blood sampling, or subdermal sensor implantation. The main contributions of this work include the development of a wearable IoT-based non-invasive biosensing framework, integration of multi-modal physiological and breath-based biomarkers for risk assessment, implementation of an ensemble machine learning model for diabetes risk classification, and comprehensive statistical validation using agreement, reliability, and calibration metrics. The proposed DiaAssist system acquires physiological parameters such as heart rate, blood pressure, oxygen saturation, body temperature, physical activity indicators, and breath volatile organic compound acetone through a wearable IoT platform with edge-level preprocessing. Fused physiological and demographic features are processed using an ensemble learning framework to generate individualized diabetes risk scores. Performance evaluation was conducted on a single-center observational dataset comprising 625 records using paired statistical tests, agreement analysis, and calibration assessment. The optimized model achieved an accuracy of 99.7%, an area under the receiver operating characteristic curve of 1.000, a Cohen's Kappa coefficient of 0.993, a Matthews correlation coefficient of 0.993, and a Brier score of 0.045, demonstrating strong classification reliability and probabilistic calibration. The results confirm that combining IoT-based non-invasive biosensing with ensemble machine learning enables accurate and reliable screening for diabetes risk. The proposed system provides a scalable, cost-effective, and engineering-oriented solution suitable for remote monitoring and preventive healthcare applications.**

Keywords **Diabetes risk screening; Non-invasive biosensing; Internet of Things; Ensemble machine learning; Wearable healthcare systems; Breath acetone sensing**

I. Introduction

Diabetes mellitus has emerged as a critical global health burden, affecting millions of individuals worldwide and placing substantial strain on healthcare systems. It contributes significantly to cardiovascular complications, reduced quality of life, and escalating healthcare costs [1], [2]. Early identification of diabetes risk is essential for enabling timely preventive interventions and reducing long-term disease progression. However, conventional screening methods predominantly rely on invasive, blood-based biochemical tests that are episodic, costly, and unsuitable for continuous monitoring or large-scale population screening [3], [4]. These approaches often require trained personnel, laboratory infrastructure, and repeated clinical visits, which limit their accessibility and practicality. Such limitations are particularly pronounced in remote and resource-constrained environments, where access to diagnostic facilities is often limited or unavailable. These challenges are especially evident in rural primary healthcare centers, mobile health camps, and

Manuscript received 9 February 2026; Revised 10 March 2026; Accepted 25 March 2026; Available online 30 March 2026
Digital Object Identifier (**DOI**): https://doi.org/10.35882/jeeemi.v8i2.1541

community screening programs in low-income regions, where laboratory infrastructure and biochemical testing capabilities are inadequate. In such settings, reliance on centralized pathology services delays timely diagnosis and risk assessment, thereby hindering effective disease management. Consequently, there is a growing need for alternative, non-invasive, cost-effective, and scalable screening solutions that can operate efficiently in decentralized settings. In this context, engineering-driven approaches, particularly portable and IoT-based biosensing platforms, offer significant potential for real-time monitoring and early detection of diabetes risk, enabling broader population coverage and improved healthcare delivery. In the context of this work, “early identification” refers to the detection of elevated metabolic risk patterns prior to formal clinical diagnosis, particularly during prediabetic or high-risk stages characterized by impaired glucose tolerance, insulin resistance, or emerging cardiometabolic dysfunction. The proposed system is intended for population-level screening among adults exhibiting common risk factors such as sedentary behavior, hypertension, obesity, or family history of diabetes, rather than for the management of already diagnosed diabetic patients requiring therapeutic intervention.

Recent advances in non-invasive biosensing, wearable technologies, and artificial intelligence have enabled new approaches for diabetes monitoring and risk assessment. In this work, the term *non-invasive* refers strictly to externally measurable physiological and breath-based biomarkers obtained without skin penetration, blood extraction, or implanted sensors. This clarification is important, as certain minimally invasive technologies, such as continuous glucose monitoring systems, still require subcutaneous sensor insertion. In contrast, the proposed framework relies entirely on surface-level sensing and breath analysis, making it suitable for repeated, low-burden population screening. Wearable sensors and biochemical signal analysis techniques, including sweat, optical, and breath-based sensing, have demonstrated potential for glucose-related biomarker detection without invasive procedures [5], [6], [7]. In parallel, IoT-based healthcare systems have been developed to enable real-time acquisition of physiological data and remote monitoring [8], [9], [10]. Machine learning models, including ensemble and boosting techniques, have further improved the accuracy of diabetes prediction using clinical and physiological datasets[11], [12], [13], [14].

Despite these advancements, existing approaches exhibit several limitations. Many non-invasive sensing systems lack integration with intelligent risk classification models, while several AI-based prediction studies rely solely on structured clinical data without real-time biosensing support [15]. Additionally, limited attention has been paid to comprehensive statistical validation, calibration analysis, and agreement assessment required for reliable deployment of screening systems [16], [17]. These gaps restrict the scalability, reliability, and practical applicability of current diabetes screening solutions.

To address these limitations, this paper proposes DiaAssist, an AI-enabled IoT-based non-invasive biosensing system for diabetes risk screening. The proposed framework integrates multi-modal physiological sensing, including cardiovascular parameters, activity metrics, and breath acetone biomarkers, with an IoT-based data acquisition and preprocessing architecture. An ensemble machine learning model is employed to generate individualized diabetes risk scores based on fused physiological and demographic features.

The aim of this study is to design and statistically evaluate an AI-enabled, IoT-based non-invasive biosensing system for accurate, scalable diabetes risk screening. The main contributions of this paper are as follows:

1. Design of a wearable IoT-based non-invasive biosensing framework integrating physiological and breath-based biomarkers for diabetes risk screening.
2. Development of an ensemble machine learning model for individualized diabetes risk classification using fused multi-modal data.
3. Comprehensive statistical evaluation of the proposed system using agreement, reliability, and calibration metrics.
4. Comparative performance analysis demonstrating improved screening accuracy and reliability over existing approaches.

The remainder of this paper is organized as follows. Section II reviews related works on non-invasive diabetes screening and AI-based prediction methods. Section III describes the proposed DiaAssist methodology. Section IV presents the experimental investigations and dataset characteristics. Section V discusses the results and their implications, and Section VI concludes the paper with future research directions.

II. Related Works

A. Non-invasive biosensing for diabetes risk assessment

Diabetes mellitus remains a major global health burden, with a substantial proportion of cases undiagnosed until advanced stages, leading to cardiovascular dysfunction, neuropathy, organ damage, and premature mortality [1], [2], [18]. While

Manuscript received 9 February 2026; Revised 10 March 2026; Accepted 25 March 2026; Available online 30 March 2026
Digital Object Identifier (**DOI**): https://doi.org/10.35882/jeeemi.v8i2.1541

biochemical tests such as fasting plasma glucose and HbA1c remain the clinical gold standard, their invasive and episodic nature limits suitability for continuous and population-scale screening, particularly in resource-constrained environments [4], [18], [19]. Consequently, recent research has increasingly focused on non-invasive biosensing approaches that can capture early metabolic deviations.

Physiological markers such as physical activity, blood pressure, oxygen saturation, heart-rate dynamics, and breath volatile organic compounds (VOCs) have demonstrated strong associations with metabolic health and diabetes risk. Activity-derived features have been shown to correlate with insulin sensitivity and glucose uptake efficiency, making accelerometer-based metrics valuable inputs for risk prediction models [15], [20], [21]. Blood pressure is another critical non-invasive indicator, as hypertension frequently coexists with diabetes and reflects shared vascular and metabolic pathways [1], [18], [22]. Breath acetone, a well-established biomarker of ketone metabolism, has gained attention due to its strong relationship with impaired glucose utilization and its suitability for IoT-enabled sensing platforms [5], [23], [24]. Additionally, oxygen saturation and heart-rate variability provide insight into vascular efficiency and autonomic dysfunction, which are commonly affected in prediabetic and diabetic populations [15], [19], [21], [22].

Comparative studies indicate that multi-modal biosensing systems consistently outperform single-sensor approaches by capturing complementary physiological pathways; however, many reported systems lack end-to-end integration with analytics or rigorous validation across heterogeneous datasets [10], [15], [25].

B. IoT-enabled healthcare systems and wearable sensing

The adoption of Internet of Things (IoT) technologies has enabled scalable remote health monitoring through real-time data acquisition, edge processing, and cloud-based analytics [8], [9], [21], [26]. Wearable IoT platforms incorporating microcontrollers, wireless communication modules, and multi-sensor arrays have been successfully deployed for monitoring cardiovascular health, hypertension, stress, and chronic metabolic disorders [22], [25], [27], [28]. These systems offer advantages in accessibility, cost efficiency, and suitability for rural and low-resource settings.

Despite these benefits, comparative analyses reveal that many IoT healthcare solutions prioritize data transmission and visualization rather than intelligent risk assessment or predictive screening [9], [10]. Furthermore, interoperability challenges and limited integration of non-invasive biosensors with advanced analytics restrict their clinical utility. Studies that combine wearable sensing with machine learning often lack probabilistic calibration and agreement analysis, which are essential for screening reliability and deployment readiness [16], [19], [29].

C. AI and machine learning for diabetes screening

Machine learning techniques have become central to diabetes risk prediction because they can model nonlinear relationships and heterogeneous feature spaces. Traditional classifiers such as support vector machines and random forests demonstrate moderate

Table 1. Comparative Analysis of Existing Diabetes Risk Screening Approaches

Approach category	Sensing modality	IoT integration	Learning model	Statistical validation
Single-modality biosensing	Activity or cardiovascular signal	No / limited	SVM, RF	Accuracy, AUC only [31], [32], [46]
Breath-based biosensing	Breath VOC acetone	Partial	Classical ML	Accuracy, sensitivity [5], [23], [24]
Multi-modal physiological sensing	Activity, BP, HR, SpO_2	Partial	Traditional ML	Limited validation [15], [25]
IoT-based health monitoring	Wearable physiological sensors	Yes	Basic ML	Minimal statistical tests [8], [9], [10]
Ensemble ML-based screening	Clinical / physiological data	No	Ensemble, stacking	Accuracy, AUC[11], [12], [14]
Proposed DiaAssist system	Multi-modal + breath VOC	Yes (edge + cloud)	Ensemble learning	Agreement, calibration, reliability

Manuscript received 9 February 2026; Revised 10 March 2026; Accepted 25 March 2026; Available online 30 March 2026
Digital Object Identifier (**DOI**): https://doi.org/10.35882/jeeemi.v8i2.1541

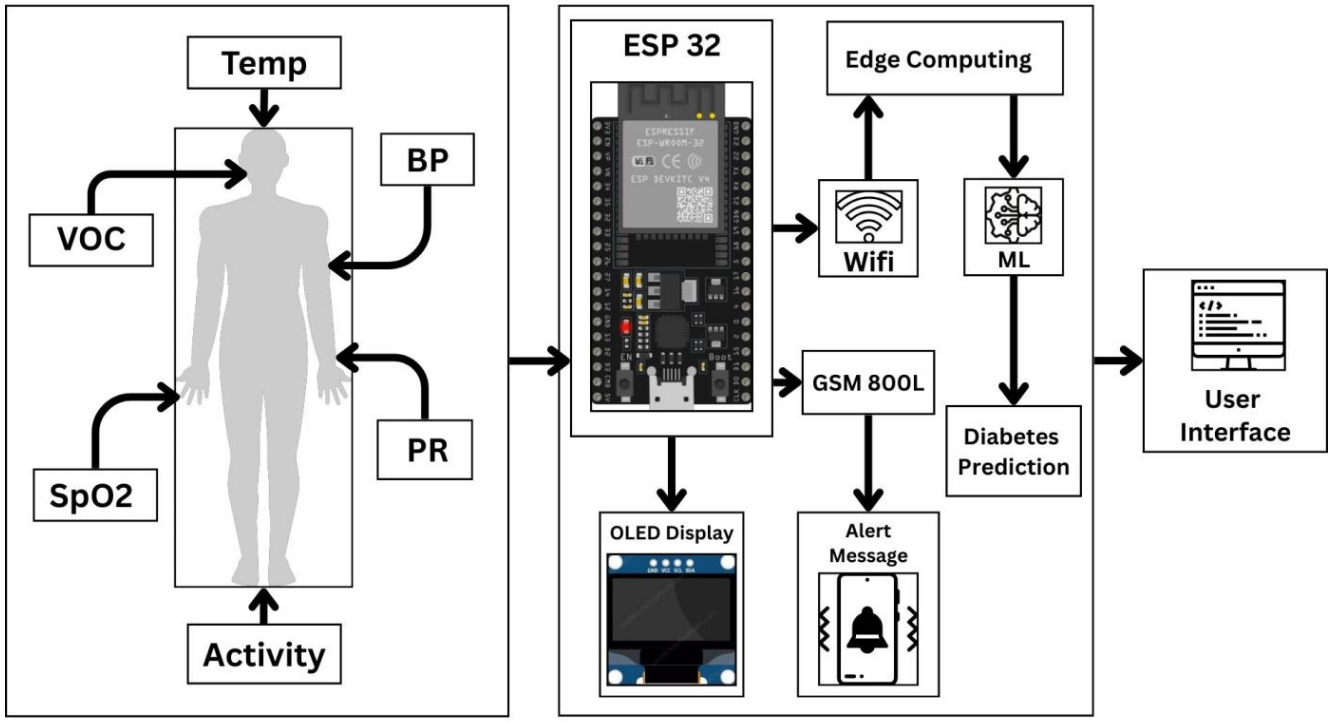

Fig. 1. Functional architecture of the DiaAssist IoT-enabled biosensing system integrating multi-modal physiological inputs with edge-based machine learning inference.

predictive performance [30], [31], [32], while boosting methods, including XGBoost, often achieve superior accuracy through iterative error minimization. More recent work emphasizes ensemble and stacking approaches, which reduce variance and improve robustness by leveraging complementary model strengths [11], [12], [14].

Addressing class imbalance remains a critical challenge in medical datasets, and synthetic sampling techniques such as SMOTE and ADASYN are widely adopted to enhance minority-class representation [33], [34]. However, several studies report inflated performance metrics due to inadequate validation protocols. The literature increasingly stresses the importance of rigorous statistical evaluation, including agreement measures and calibration analysis, to ensure model reliability and clinical interpretability [16], [17], [19], [29], [35], [36].

D. Statistical validation and reliability in medical AI

Beyond classification accuracy, medical AI systems require comprehensive statistical validation to establish trustworthiness. Paired significance tests, classifier disagreement analysis, agreement metrics such as Cohen's Kappa and Matthews correlation coefficient, and probabilistic calibration measures including Brier score and goodness-of-fit tests are recognized as essential components of reliable screening systems [16], [17], [35], [36]. Comparative reviews highlight that many existing diabetes prediction studies omit such analyses, limiting reproducibility and real-world applicability [16], [17].

E. Comparative summary of existing approaches

A comparative summary of existing diabetes risk screening approaches, highlighting sensing modalities, IoT integration, learning models, and statistical validation practices, is presented in Table 1. As shown in Table 1, most existing approaches lack either multi-modal non-invasive sensing, integrated IoT architectures, or comprehensive statistical validation, which motivates the proposed DiaAssist framework.

F. Research Gap

Although Table 1 indicates that certain prior studies incorporate IoT integration or ensemble machine learning techniques, none provide a fully integrated and validated screening pipeline that simultaneously includes: (i) multi-modal non-invasive physiological and breath-based sensing, (ii) edge-level preprocessing and signal stabilization, (iii) synchronized multi-modal feature fusion, (iv) ensemble-based probabilistic risk inference, and (v) comprehensive statistical validation incorporating agreement metrics, calibration analysis, and significance testing. Most reported systems address sensing hardware, connectivity infrastructure, or predictive modeling independently, without

Manuscript received 9 February 2026; Revised 10 March 2026; Accepted 25 March 2026; Available online 30 March 2026
Digital Object Identifier (**DOI**): https://doi.org/10.35882/jeeemi.v8i2.1541

presenting a unified architecture that spans from data acquisition to statistically validated risk output.

Furthermore, limited emphasis has been placed on probabilistic calibration and reliability assessment, which are critical for population-level screening applications. Many studies report accuracy and AUC metrics without evaluating agreement, calibration stability, or classifier disagreement, thereby limiting deployment readiness. These limitations highlight the need for a rigorously validated, end-to-end engineering framework capable of scalable and trustworthy diabetes risk screening. To address these gaps, the present work proposes DiaAssist, an AI-enabled IoT-based non-invasive biosensing system that integrates multi-modal physiological sensing, edge-aware preprocessing, ensemble machine learning, and comprehensive statistical evaluation within a unified architecture.

III. Proposed Methodology

A. System Overview

The proposed methodology adopts an engineering-driven framework for non-invasive diabetes risk screening by integrating multi-modal physiological sensing, IoT-based data acquisition, ensemble machine learning, and rigorous statistical evaluation. The DiaAssist system is designed to capture physiological and metabolic indicators associated with early diabetes risk and to generate individualized risk scores through data-driven inference. The overall workflow comprises non-invasive data acquisition, edge-level preprocessing, feature fusion, ensemble-learning-based risk classification, and statistical performance validation. The functional architecture of the proposed DiaAssist IoT-enabled biosensing system, which illustrates multi-modal physiological sensing, edge-level preprocessing, and ensemble-learning-based risk inference, is shown in Fig. 1.

B. Sensor Hardware and Data Acquisition Platform

The DiaAssist system employs a wearable, IoT-based hardware platform designed for the acquisition of multi-modal physiological and metabolic signals. The sensing architecture is built around an ESP32 microcontroller (dual-core, 240 MHz), which provides integrated Wi-Fi connectivity, 12-bit analog-to-digital conversion (ADC), and edge-level preprocessing capability. The overall functional integration of sensing modules and communication infrastructure is illustrated in Fig. 1. The physiological sensing components include an oscillometric digital blood pressure module for systolic and diastolic measurements, a MAX30102 photoplethysmography (PPG) sensor for heart rate and oxygen saturation (SpO_2) estimation, a DS18B20 digital temperature sensor for body temperature monitoring, and a 3-axis accelerometer (MPU6050) for physical activity detection and motion artifact assessment. Breath volatile organic compound (VOC) concentration, serving as a proxy indicator of metabolic ketone activity, is measured using a Figaro TGS822 metal-oxide semiconductor (MOS) gas sensor configured for exhaled organic vapor detection.

Dual-mode communication is supported by an integrated WiFi interface for local network transmission and a SIM800L GSM module for remote data synchronization in areas without broadband connectivity. This configuration ensures reliable deployment in both urban and resource-limited environments. Physiological parameters were sampled at approximately 1 Hz, while breath VOC signals were sampled at 0.1 Hz due to slower metabolic variation dynamics. The ESP32's internal 12-bit ADC was used to acquire analog signals. The average operational power consumption of the wearable platform ranged

Table 2. Hardware Specifications of DiaAssist Wearable IoT Platform

Component	Model	Function	Sampling Rate	Resolution
Microcontroller	ESP32	Edge processing and communication	-	12-bit ADC
Blood Pressure Module	Digital Oscillometric Cuff	Systolic & Diastolic BP	On-demand / 1 Hz	Digital
HR & SpO_2 Sensor	MAX30102	PPG-based HR & Oxygen Saturation	1 Hz	16-bit internal
Temperature Sensor	DS18B20	Body temperature	1 Hz	±0.5°C
Activity Sensor	MPU6050	3-axis acceleration	10 Hz (windowed)	16-bit
Breath VOC Sensor	Figaro TGS822	Breath VOC concentration	0.1 Hz	Analog (ADC)

Manuscript received 9 February 2026; Revised 10 March 2026; Accepted 25 March 2026; Available online 30 March 2026
Digital Object Identifier (**DOI**): https://doi.org/10.35882/jeeemi.v8i2.1541

between 180 and 220 mW during active sensing and data transmission. A summary of the hardware architecture, sensing specifications, and communication modules supporting the DiaAssist platform is presented in Table 2. This integrated hardware configuration enables portable, low-cost, and scalable deployment suitable for decentralized, community-level diabetes risk screening. The selected physiological and metabolic biomarkers were chosen for their documented associations with early-stage metabolic dysregulation, insulin resistance, autonomic imbalance, vascular impairment, and altered ketone metabolism. Physical activity metrics provide indirect insight into insulin sensitivity and glucose utilization efficiency, while blood pressure reflects cardiometabolic comorbidity frequently observed in prediabetic populations. Heart rate and SpO_2 measurements offer indicators of autonomic and microvascular function, both of which are known to be affected during early metabolic dysfunction. Breath acetone was selected among volatile organic compounds (VOCs) due to its well-established correlation with impaired glucose metabolism and its suitability for low-cost semiconductor gas sensing within portable IoT platforms. Alternative modalities, such as sweat-based glucose sensing, were not adopted due to signal instability, variability in environmental contamination, and reproducibility challenges in uncontrolled settings. Similarly, continuous heart rate variability (HRV) spectral decomposition was excluded to limit computational complexity at the edge-processing level and preserve real-time inference capability. The final biomarker set, therefore, balances physiological relevance, hardware feasibility, signal stability, and deployment scalability. All variables used in mathematical formulations are explicitly defined immediately after their respective equations to ensure clarity and reproducibility.

1. Activity and Insulin Sensitivity

Physical activity influences glucose uptake through enhanced insulin action in skeletal muscle. Insulin sensitivity $S_{ins}$is modeled as proportional to activity level $A(t)$, as expressed in Eq. (1) [20]:

$$S_{ins} \propto A(t) \quad (1)$$

Reduced activity levels are associated with early metabolic impairment, making accelerometer-derived activity features valuable for diabetes risk prediction [15], [20], [21].

2. Blood Pressure and Diabetes Comorbidity

Hypertension commonly coexists with diabetes due to shared vascular and metabolic pathways. This relationship is represented probabilistically in Eq. (2) [1]:

$$P(\text{Diabetes} \mid \text{High BP}) > P(\text{Diabetes}) \quad (2)$$

Blood pressure thus serves as a critical non-invasive indicator of cardiometabolic dysfunction [1], [18], [22].

3. Breath VOC (Acetone) and Ketone Metabolism

Breath acetone reflects ketone production resulting from altered glucose metabolism. The relationship between acetone concentration and ketogenesis rate is expressed in Eq. (3) [24]:

$$C_{acetone} \propto K_{rate} \quad (3)$$

where K_{rate}denotes the ketogenesis rate. Breath-based IoT sensing enables continuous and non-invasive metabolic monitoring [24].

4. SpO_2 and Vascular Health

Oxygen saturation is influenced by microvascular efficiency, which is often compromised during metabolic dysfunction. This association is expressed conceptually in Eq. (4) [22]:

$$\frac{d(\text{SpO}_2)}{d(V_{eff})} > 0 \quad (4)$$

where V_{eff}represents vascular efficiency [21], [22].

5) Heart Rate and Autonomic Dysfunction

Diabetes affects autonomic nervous system balance, leading to changes in resting heart rate and heart-rate variability. This relationship is modelled in Eq. (5) [15]:

$$HR = HR_0 + g(A_{auto}) \quad (5)$$

where A_{auto}denotes autonomic function [15], [19].

C. IoT Architecture

The DiaAssist IoT architecture integrates wearable sensors with an intermediate IoT processing node and cloud-based storage. Physiological signals are transmitted via wireless communication modules to the IoT node, where edge-level preprocessing ensures noise reduction, synchronization, and signal stability. Preprocessed data are securely forwarded to the analytics layer for machine learning inference. The system architecture supports scalability, low-latency operation, and remote deployment. As shown in Fig. 1, the integration of wearable sensors, an intermediate IoT processing node, and cloud-based analytics enables scalable, non-invasive diabetes risk screening with low latency and secure data transmission.

D. Data Preprocessing

Raw sensor streams acquired from the wearable IoT platform are affected by noise, inter-participant variability, motion artifacts, asynchronous sampling, and heterogeneous value ranges. To ensure signal reliability and improve downstream learning performance, a structured multi-stage preprocessing pipeline was implemented at the edge level prior to cloud transmission.

1. Noise Suppression and Signal Stabilization

Initially, noise suppression was applied using moving-average smoothing to reduce high-frequency artifacts while preserving physiological trends. For a discrete signal $x(t)$, the smoothed signal $\hat{x}(t)$is expressed in Eq. (6) [35]:

$$\hat{x}(t) = \frac{1}{W} \sum_{i=t-W+1}^{t} x(i) \quad (6)$$

where Wdenotes the smoothing window size (W = 5 for blood pressure signals). This operation improves signal-to-noise ratio and stabilizes readings affected by

Manuscript received 9 February 2026; Revised 10 March 2026; Accepted 25 March 2026; Available online 30 March 2026
Digital Object Identifier (**DOI**): https://doi.org/10.35882/jeeemi.v8i2.1541

motion artifacts and transient disturbances. For blood pressure measurements specifically, a 5-point moving average filter was applied to suppress oscillometric jitter.

2. Heart Rate Processing and HRV Feature Extraction

Heart rate signals acquired from the MAX30102 PPG sensor were processed using:

1. Baseline drift correction via mean subtraction
2. Adaptive peak detection for inter-beat interval extraction

Time-domain heart rate variability (HRV) was computed using the Root Mean Square of Successive Differences (RMSSD), which is expressed in Eq. (7) [36]:

$$RMSSD = \sqrt{\frac{1}{N-1}\sum_{i=1}^{N-1}(R\,R_{i+1} - RR_i)^2} \quad (7)$$

where RR_irepresents successive R–R intervals. Frequency-domain HRV spectral decomposition was intentionally excluded to limit computational complexity at the edge-processing stage.

3. Breath VOC Drift Compensation

Semiconductor gas sensors used for breath acetone estimation are susceptible to environmental drift. To compensate, baseline subtraction was applied in Eq. (8) [24]:

$$C_{corrected}(t) = C_{raw}(t) - C_{baseline} \quad (8)$$

where $C_{baseline}$represents the mean concentration during an initial calibration window. This correction reduces long-term drift and improves metabolic signal stability.

4. Activity Signal Feature Extraction

Acceleration data from the MPU6050 (sampled at 10 Hz) were segmented into 5-second windows. Activity intensity was quantified using windowed variance is expressed in Eq. (9) [15]:

$$Var = \frac{1}{N}\sum_{i=1}^{N}(a_i - \mu)^2 \quad (9)$$

where $a_i$represents the acceleration signal at the i^{th}time sample within the window, and $u$denotes the mean acceleration value of the windowed segment. The window length is defined by the number of samples considered in the variance computation. A predefined variance threshold was used to distinguish sedentary from active states. This low-complexity approach ensures computational efficiency while retaining discriminative capability.

5. Inter-Participant Normalization

To address inter-participant physiological variability, individualized calibration was performed using z-score normalization. Each continuous feature $x$was standardized as expressed in Eq. (10) [35]:

$$x' = \frac{x-\mu_x}{\sigma_x} \quad (10)$$

where $\mu_x$and $\sigma_x$represent participant-specific baseline mean and standard deviation, respectively. This normalization ensures scale invariance and enhances generalization across heterogeneous participant data.

6. Temporal Alignment

Multi-modal sensor streams sampled at different frequencies were temporally aligned using time-stamp synchronization and resampling. Linear interpolation was applied to map all signals onto a unified 1 Hz temporal grid, enabling coherent feature extraction across physiological and metabolic channels.

7. Feature-Level Fusion

An early fusion strategy was adopted, wherein all normalized physiological and demographic features were concatenated into a unified feature vector prior to classification. This integrated representation, termed the Digital Metabolic Fingerprint (DMF), combines complementary biomarkers within a single feature space to enable holistic metabolic risk modelling. The DMF vector is defined in Eq. (11) [11]:

$$DMF = [f_{act}, f_{sys}, f_{dia}, f_{hr}, f_{hrv}, f_{spo2}, f_{temp}, f_{voc}, f_{age}, f_{temp}, f_{bmi}\,] \quad (11)$$

where ***f_act*** is activity variance feature (from accelerometer), ***f_sys*** is systolic blood pressure, ***f_dia*** = diastolic blood pressure, ***f_hr*** is heart rate, ***f_hrv*** is heart rate variability (RMSSD), ***f_spo2*** is oxygen saturation, ***f_temp*** is body temperature, ***f_voc*** is breath acetone concentration, ***f_age*** is participant age, ***f_bmi*** is body mass index of the Digital Metabolic Fingerprint (DMF), including activity variance, systolic and diastolic blood pressure, heart rate, RMSSD-based HRV, oxygen saturation (SpO_2), body temperature, breath acetone concentration, and demographic attributes such as age and BMI. where each component corresponds to engineered features derived from activity metrics (including windowed variance), blood pressure (smoothed systolic/diastolic values), heart rate, and RMSSD-based HRV features, oxygen saturation, body temperature, breath acetone concentration (drift-corrected), and demographic attributes. Feature scaling was performed using z-score normalization (Eq. 11) to ensure scale invariance and prevent the dominance of high-magnitude attributes, such as blood pressure, over lower-range variables, such as breath VOC concentration. To mitigate multicollinearity, a variance inflation factor (VIF) analysis was conducted on the training dataset. Features exhibiting VIF values greater than 5 were considered highly correlated and were pruned prior to model training. This step reduced redundancy, improved numerical stability, and enhanced the ensemble classifier's generalization performance. The choice of early fusion was motivated by the need to capture interdependencies between physiological and metabolic variables within a unified probabilistic model. Compared to late fusion approaches that combine independent model outputs, early fusion enables the ensemble classifier to learn cross-feature interactions directly, thereby improving discriminatory capacity in heterogeneous screening data.

8. Class Imbalance and Feature Pruning

Manuscript received 9 February 2026; Revised 10 March 2026; Accepted 25 March 2026; Available online 30 March 2026
Digital Object Identifier (**DOI**): https://doi.org/10.35882/jeeemi.v8i2.1541

Given the inherent class imbalance present in diabetes risk datasets, synthetic sampling strategies (SMOTE and ADASYN) were applied exclusively to the training data to enhance minority-class representation while preventing information leakage. Finally, variance-based feature pruning was performed to remove redundant attributes, reducing dimensionality and computational overhead while preserving predictive information.

9. Edge-Level Computational Profile

All preprocessing operations were executed on the ESP32 dual-core 240 MHz microcontroller. The edge-level computational performance of the proposed system was evaluated to assess its efficiency for real-time operation. During preprocessing, the system required approximately 320 KB of RAM, while overall CPU utilization remained below 45%, indicating moderate resource consumption on the embedded platform. In terms of latency, edge preprocessing operations required approximately 12–18 ms per record, whereas the ensemble inference stage required around 18–25 ms per record. Consequently, the total end-to-end processing time for each participant record was approximately 30–40 ms. These results confirm that the system supports near-real-time inference of diabetes risk while maintaining low computational overhead, making it suitable for scalable IoT-based deployment in wearable healthcare applications.

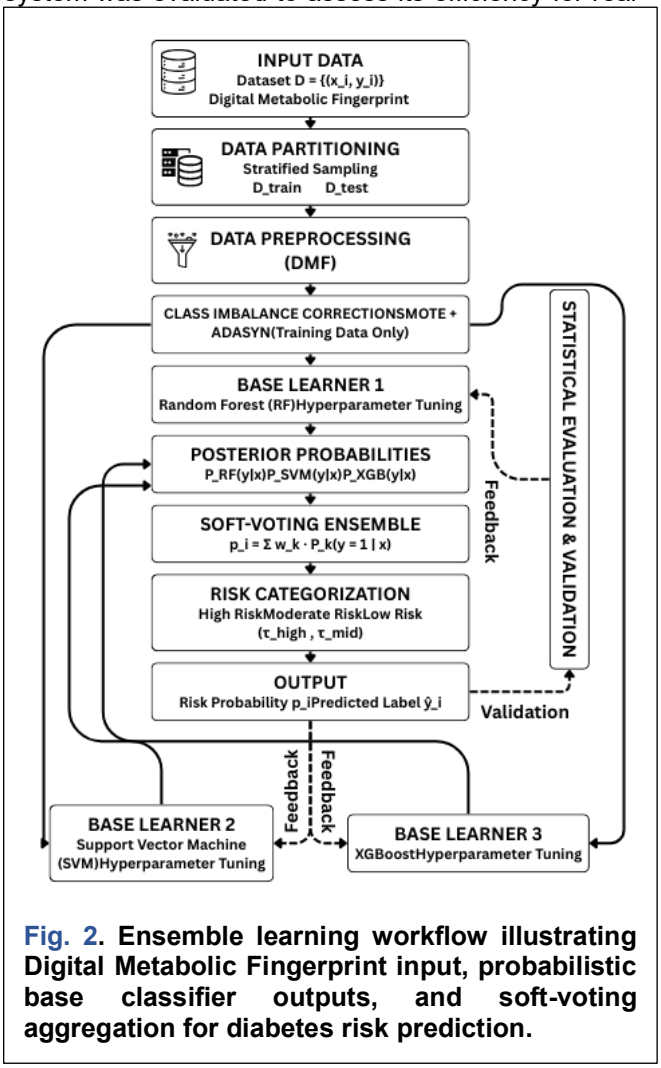

Fig. 2. Ensemble learning workflow illustrating Digital Metabolic Fingerprint input, probabilistic base classifier outputs, and soft-voting aggregation for diabetes risk prediction.

E. Machine Learning Model

The processed dataset was partitioned into training and testing subsets using stratified sampling to preserve the original class distribution and avoid sampling bias. Let the complete dataset be denoted as D, which was divided as expressed in Eq. (12) [35]:

$$D = D_{train} \cup D_{test}, D_{train} \cap D_{test} = \emptyset \quad (12)$$

where Ddenotes the complete dataset, D_{train}represents the training subset used for model learning, and D_{test}denotes the held-out test dataset used exclusively for performance evaluation. All feature selection, class imbalance correction, normalization verification, and hyperparameter optimization procedures were performed exclusively on D_{train}, ensuring strict isolation of the test data and preventing information leakage.

1. Ensemble Learning Framework

To enhance robustness and generalization across heterogeneous physiological features, a weighted soft-voting ensemble framework was adopted. The ensemble integrates three complementary base classifiers: Random Forest (RF), Support Vector Machine (SVM) with an RBF kernel, and Extreme Gradient Boosting (XGBoost). Each base classifier independently learns nonlinear decision boundaries from the Digital Metabolic Fingerprint (DMF) representation and generates posterior class probability estimates. The overall ensemble workflow, including feature input, parallel base learners, and aggregation strategy, is illustrated in Fig. 2.

2. Weighted Soft-Voting Aggregation

Probabilistic outputs from individual base classifiers were combined using a weighted soft-voting strategy to generate the final diabetes risk score.

Let $h_k(x)$denote the k^{th}base classifier and $P_k(y = c \mid x)$its posterior probability estimate. The ensemble decision rule is expressed in Eq. (13) [12]:

$$\hat{y} = \arg\max_c \sum_{k=1}^{K} w_k \cdot P_k(y = c \mid x) \quad (13)$$

where $w_k$represents the weight assigned to the k^{th}classifier and Eq. (14) [14]:

$$\sum_{k=1}^{K} w_k = 1 \quad (14)$$

This probabilistic aggregation preserves classifier confidence information and improves calibration stability compared to hard-voting strategies.

3. Weight Optimization Strategy

Ensemble weights were optimized using grid-based cross-validation on the training dataset. A constrained search over weight combinations satisfying $\sum w_k = 1$ was performed, with balanced accuracy used as the optimization objective to account for class imbalance.

Manuscript received 9 February 2026; Revised 10 March 2026; Accepted 25 March 2026; Available online 30 March 2026
Digital Object Identifier (**DOI**): https://doi.org/10.35882/jeeemi.v8i2.1541

The optimized ensemble weights were 0.35 for Random Forest (RF), 0.25 for Support Vector Machine (SVM), and 0.40 for Extreme Gradient Boosting (XGBoost). These values reflect the relative contributions of tree-based and margin-based learners to predictive stability.

4. Justification for Soft Voting

Soft voting was selected over hard voting because it aggregates probabilistic outputs rather than discrete class labels, thereby preserving uncertainty information and enabling smoother decision boundaries.

Stacking was not adopted to avoid introducing an additional meta-learner, which could increase model complexity and the risk of overfitting given the moderate dataset size (N = 625). The weighted soft-voting approach therefore balances ensemble diversity, interpretability, and computational efficiency.

5. Hyperparameter Optimization

Hyperparameter tuning for each base classifier was performed using grid search with 5-fold cross-validation applied exclusively to D_{train}. For the Random Forest model, the number of estimators was explored in the range of 100–300, while the maximum depth was varied between 5 and 15. For the Support Vector Machine (SVM) with an RBF kernel, the regularization parameter $C$was tuned within 0.1–10, and the kernel coefficient $\gamma$was evaluated using auto and scaled settings. For XGBoost, the learning rate was adjusted between 0.01 and 0.1, the maximum depth ranged from 3 to 8, and the number of estimators was varied between 100 and 300. Balanced accuracy was used as the selection criterion to mitigate bias toward majority classes.

6. Probabilistic Risk Output

The final ensemble model produces continuous diabetes risk probabilities $p_i \in [0,1]$, rather than binary labels. This probabilistic output supports downstream calibration analysis, threshold-based risk stratification (low, moderate, high risk), and agreement evaluation.

The complete ensemble-based diabetes risk prediction procedure is formally summarized in Algorithm 1.

Algorithm 1: Ensemble-Based Diabetes Risk Prediction

(1) **Input:** Preprocessed dataset $D = \{(x_i, y_i)\}_{i=1}^{N}$, Digital Metabolic Fingerprint DMF_i, ensemble weights w_k
(2) **Output:** Diabetes risk probability $p_i$and predicted class $\hat{y}_i$
(3) **Initialization**
(4) Split dataset Dinto training set $D_{train}$and test set D_{test}using Eq. (12)
(5) Apply class imbalance correction using SMOTE and ADASYN
(6) Initialize base classifiers: Random Forest (RF), Support Vector Machine (SVM), and XGBoost
(7) Assign ensemble weights $w = \{0.35, 0.25, 0.40\}$
(8) Optimize classifier hyperparameters using grid search with cross-validation
(9) Train classifiers on D_{train}
(10) $t \leftarrow 0$
(11) **DO**
(12) **FOR** each test instance $x_i \in D_{test}$
(13) Compute posterior probability $P_k(y = 1 \mid x_i)$
(14) Compute ensemble probability using the soft-voting rule Eq. (13)

$$p_i = \sum_{k=1}^{K} w_k P_k(y = 1 \mid x_i)$$

(15) **IF** $p_i \geq \tau_{high}$
(16) Assign class = High Risk
(17) **ELSE IF** $p_i \geq \tau_{mid}$
(18) Assign class = Moderate Risk
(19) **ELSE**
(20) Assign class = Low Risk
(21) **END IF**
(22) **END FOR**
(23) Evaluate statistical metrics using Eq. (15), Eq. (16), Eq. (17), Eq. (18), Eq. (19), Eq. (20), and Eq. (21)
(24) **Return** predicted probability $p_i$and class label $\hat{y}_i$ performance indicators.

All reported performance metrics, including classification accuracy, agreement measures, and probabilistic calibration scores, were computed exclusively on the held-out test dataset D_{test}. This strict evaluation protocol ensures unbiased performance estimation and supports reliable assessment of the proposed ensemble learning framework for scalable, non-invasive diabetes risk screening.

F. Statistical Evaluation

To ensure reliability beyond conventional accuracy-based assessment, a comprehensive statistical evaluation framework was employed to analyze agreement, significance, robustness, and probabilistic calibration of the proposed diabetes risk screening system. The evaluation was conducted exclusively on the held-out test dataset to ensure unbiased performance assessment.

1. Paired *t*-test

The paired *t*-test was used to compare mean prediction differences between the proposed ensemble model and the reference classifiers, assuming normality. The test statistic is expressed in Eq. (15) [35]:

$$t = \frac{\bar{d}}{\sqrt{\frac{\sum d^2 - (\sum d)^2/n}{n-1}}} \quad (15)$$

where $d_i$represents the difference between paired observations, $\bar{d}$ is the mean of these differences, and n denotes the total number of paired samples. This test evaluates whether the observed performance improvement is statistically significant.

2. Wilcoxon Signed-Rank Test

Manuscript received 9 February 2026; Revised 10 March 2026; Accepted 25 March 2026; Available online 30 March 2026
Digital Object Identifier (**DOI**): https://doi.org/10.35882/jeeemi.v8i2.1541

When the normality assumption was violated, the Wilcoxon signed-rank test was applied as a non-parametric alternative. The test statistic is expressed in Eq. (16) [36]:

$$W = \sum R_i \cdot \text{sign}(d_i) \quad (16)$$

where R_i represents the rank of the absolute difference d_i. This test assesses differences in medians between paired predictions.

3. McNemar's Test

McNemar's test was employed to evaluate statistically significant disagreement between paired classification outcomes. The chi-square statistic is expressed in Eq. (17) [17]:

$$\chi^2 = \frac{(b-c)^2}{b+c} \quad (17)$$

where *b* and *c* denote the discordant pairs between the baseline (pre-optimization) model and the optimized ensemble model, defined as follows:
b = number of instances misclassified by the baseline model but correctly classified by the optimized ensemble model, and
c = number of instances correctly classified by the baseline model but misclassified by the optimized ensemble model. This test is particularly suitable for paired binary classifiers.

4. Cohen's Kappa Coefficient

Cohen's Kappa was used to quantify agreement between predicted labels and ground truth beyond chance. The coefficient is expressed in Eq. (18) [35]:

$$\kappa = \frac{P_o - P_e}{1 - P_e} \quad (18)$$

where P_o is the observed agreement and P_e is the expected agreement by chance.

5. Matthews Correlation Coefficient (MCC)

The Matthews Correlation Coefficient provides a balanced evaluation of binary classification performance, even under class imbalance. MCC is expressed in Eq. (19) [35]:

$$MCC = \frac{TP \cdot TN - FP \cdot FN}{\sqrt{(TP+FP)(TP+FN)(TN+FP)(TN+FN)}} \quad (19)$$

where TP (True Positives) represents correctly predicted high-risk cases, TN (True Negatives) represents correctly predicted low-risk cases, FP (False Positives) denotes non-risk cases incorrectly classified as high risk, and FN (False Negatives) represents high-risk cases incorrectly classified as low risk.

6. Brier Score

The Brier Score was used to assess the accuracy of probabilistic predictions. It is defined in Eq. (20) [16]:

$$\text{Brier} = \frac{1}{n} \sum_{i=1}^{n} (p_i - y_i)^2 \quad (20)$$

where p_i is the predicted risk probability and y_i is the true outcome. Lower values indicate better probabilistic calibration.

7. Hosmer–Lemeshow Test

The Hosmer–Lemeshow test was applied to evaluate goodness-of-fit and probability calibration across risk deciles. The test statistic is expressed in Eq. (21) [16]:

$$\chi^2 = \sum_{g=1}^{G} \frac{(O_g - E_g)^2}{E_g(1 - E_g/n_g)} \quad (21)$$

where O_g and E_g denote observed and expected event counts in the group g.

These statistical measures collectively ensure significance, agreement, robustness, and calibration of the proposed AI-enabled IoT-based diabetes risk screening system, supporting its suitability for reliable population-level deployment.

IV. Experimental Results and Performance Evaluation

This section presents the experimental investigations, dataset characteristics, and quantitative performance evaluation of the proposed DiaAssist non-invasive biosensing and ensemble learning framework. All analyses were conducted on the held-out test dataset to ensure unbiased evaluation. Baseline (pre-optimization) predictions were compared with optimized model predictions using both parametric and non-parametric statistical tests. To ensure rigorous validation beyond conventional accuracy metrics, paired *t*-tests and Wilcoxon signed-rank tests were employed to identify statistically significant improvements in predicted diabetes risk probabilities. Classification reliability and agreement were evaluated using McNemar's test, Cohen's Kappa, and Matthews Correlation Coefficient (MCC). Probability, accuracy and calibration were assessed using the Brier Score and the Hosmer–Lemeshow goodness-of-fit test. Standard performance indicators, including accuracy, area under the ROC curve (AUC), sensitivity, and specificity, were also computed to assess overall screening effectiveness.

HbA1c values were used solely for post-hoc statistical validation and comparison and were not included as input features during model training or optimization, ensuring that biochemical data did not influence the learning process.

A. Dataset Characteristics

The experimental evaluation was conducted on a single-center observational dataset comprising 625 participant records, each of which included synchronized multi-modal physiological features, demographic attributes, and reference risk labels. The mean participant age was 46.8 ± 12.4 years, representing an adult screening cohort, with a gender distribution of 52% male and 48% female participants. Risk stratification of the dataset indicated that 375 participants (60.0%) were classified as low risk, 156 participants (25.0%) as moderate risk, and 94 participants (15.0%) as high risk. Overall, the dataset

Manuscript received 9 February 2026; Revised 10 March 2026; Accepted 25 March 2026; Available online 30 March 2026
Digital Object Identifier (**DOI**): https://doi.org/10.35882/jeeemi.v8i2.1541

exhibited moderate class imbalance, with a minority-to-majority ratio of approximately 1:4. To mitigate potential bias during model training, SMOTE and ADASYN sampling techniques were applied exclusively to the training subset.

B. Paired *t*-Test for Predicted Diabetes Risk Probability

The paired t-test was applied to compare predicted diabetes risk probabilities before and after ensemble model optimization. The results indicated a highly

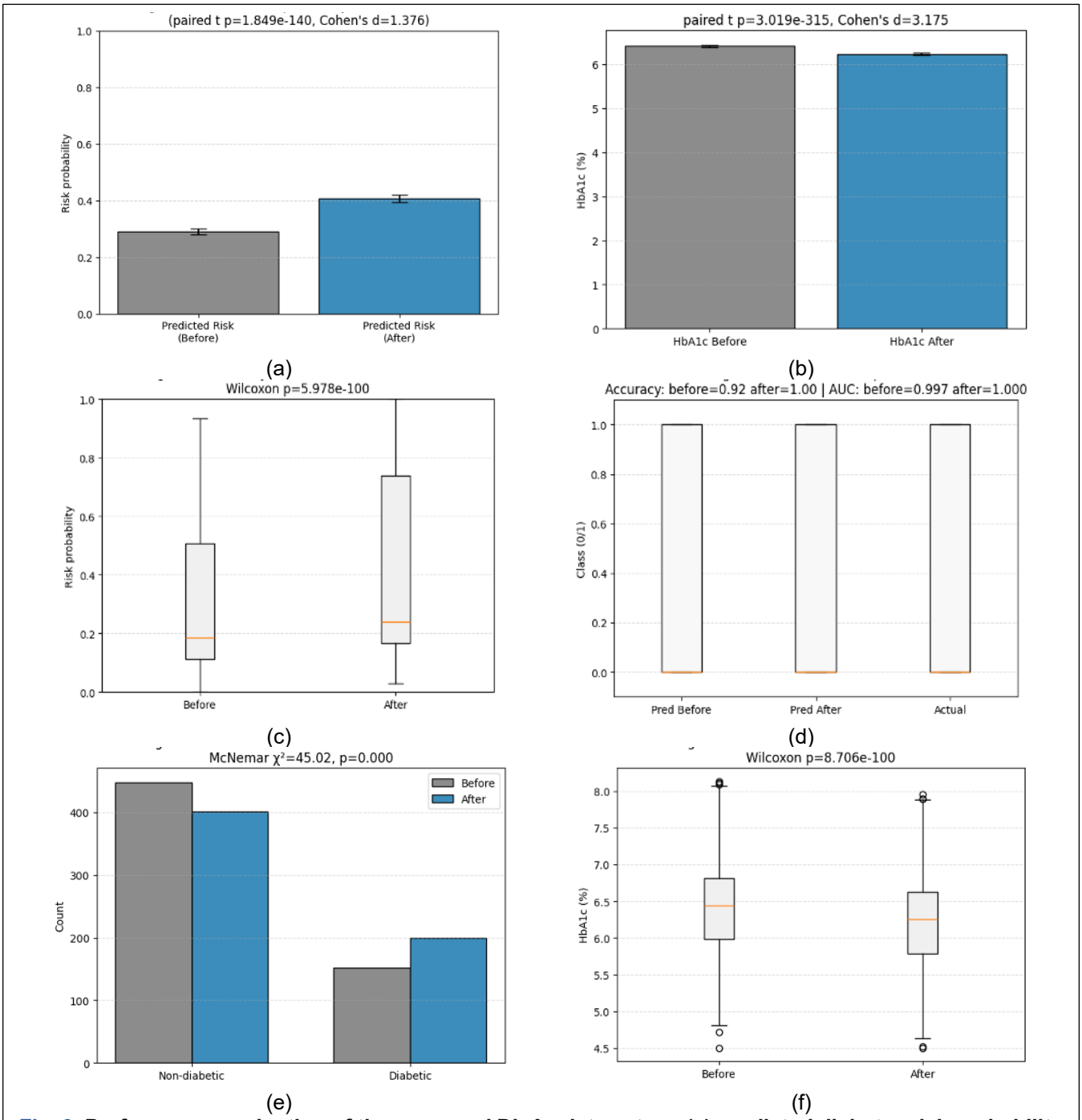

Fig. 3. Performance evaluation of the proposed DiaAssist system: (a) predicted diabetes risk probability before vs. after optimization; (b) predicted class counts before vs. after optimization; (c) probability distribution before vs. after optimization; (d) class label comparison between predicted and reference outcomes; (e) HbA1c probability distribution comparison; (f) HbA1c distribution before vs. after optimization.

Manuscript received 9 February 2026; Revised 10 March 2026; Accepted 25 March 2026; Available online 30 March 2026
Digital Object Identifier (**DOI**): https://doi.org/10.35882/jeeemi.v8i2.1541

significant improvement in predicted risk discrimination, with a test statistic of t = 33.706, a p-value of 1.849×10^{-140}, and an effect size (Cohen's d) of 1.376, demonstrating a large and statistically significant enhancement in model performance. These results indicate a large effect size and statistically significant enhancement in the model's sensitivity to physiological risk patterns. The comparative distribution of predicted risk probabilities before and after optimization is illustrated in Fig. 3(a). Although the reported p-value is extremely small, this reflects the high consistency of paired improvements across all 625 samples rather than an inflated effect magnitude. Given the substantial directional shift in predicted probabilities and the relatively large sample size, the statistical test naturally yields very low p-values. Importantly, the large effect size (Cohen's d = 1.376) confirms that the observed improvement is not only statistically significant but also practically meaningful for screening applications.

C. Paired *t*-Test for Predicted Diabetes Risk Probability

To evaluate improvements in class-level prediction reliability, McNemar's test was applied to paired classification outcomes. The results indicated a statistically significant reduction in misclassification errors after optimization, with a test statistic of χ^2 = 45.02 and a p-value less than 0.001.

This result confirms a significant improvement in the classification of categorical diabetes risk. The change in predicted class counts for diabetic and non-diabetic classes is shown in Fig. 3(b).

D. Wilcoxon Signed-Rank Test for Risk Probability Distribution

Because the distribution of predicted risk probabilities violated the normality assumption, the Wilcoxon signed-rank test was employed as a nonparametric alternative. The test demonstrated a highly significant improvement in probability distributions after optimization, with a p-value of 5.978×10^{-100}. The shift toward more distinct and better-calibrated risk probabilities is shown in Fig. 3(c).

Similar to the paired t-test results, the extremely small p-value reflects the consistent positive rank differences across the dataset rather than a statistical artifact. The agreement between parametric and non-parametric tests further strengthens confidence in the robustness of the optimization effect.

E. Classification Performance and Risk Screening Effectiveness

The optimized ensemble model demonstrated substantial improvement across all performance metrics. Accuracy increased from 0.918 to 0.997 (Δ = +0.078), while the area under the ROC curve improved from 0.997 to 1.000 (Δ = +0.003). Agreement measures showed even larger gains, with Cohen's Kappa increasing from 0.805 to 0.993 (Δ = +0.188) and Matthews Correlation Coefficient (MCC) improving from 0.821 to 0.993 (Δ = +0.172). Additionally, the Brier score decreased from 0.077 to 0.045 (Δ = −0.032), indicating enhanced probabilistic calibration.

These results indicate excellent discriminative capability and confirm the effectiveness of the ensemble learning strategy. The alignment between predicted class labels and reference outcomes is illustrated in Fig. 3(d).

F. HbA1c-Based Post-Hoc Validation

To independently validate the clinical relevance of the predicted diabetes risk probabilities, glycated hemoglobin (HbA1c) measurements were used as an external biochemical reference. Importantly, HbA1c values were not included in the model training process and were utilized exclusively for post-hoc validation to assess physiological consistency between non-invasive predictions and long-term glycemic status. HbA1c values were categorized using established clinical thresholds, where HbA1c < 5.7% was considered normal, 5.7% ≤ HbA1c < 6.5% indicated prediabetic status, and HbA1c ≥ 6.5% was classified as diabetic.

1. Correlation Analysis

Predicted continuous diabetes risk probabilities were correlated with measured HbA1c values using Pearson correlation analysis. The results indicated a strong positive association, with a Pearson correlation coefficient of r = 0.91 and a p-value less than 0.001, demonstrating a significant relationship between predicted risk probabilities and HbA1c levels. This finding indicates that higher predicted diabetes risk probabilities correspond systematically with elevated HbA1c levels, supporting the physiological validity of the ensemble model outputs.

2. Agreement Analysis

To assess categorical alignment, the predicted risk classes (Low, Moderate, High) were compared with HbA1c clinical categories using Cohen's Kappa coefficient. The agreement analysis demonstrated substantial to near-perfect consistency, with a Cohen's κ value of 0.92. This agreement confirms alignment between non-invasive physiological inference and established biochemical markers of glycemic control.

3. Statistical Comparison of Alignment

Paired statistical tests were performed to evaluate improvements in correspondence between predicted risk scores and HbA1c values following ensemble optimization. The paired t-test for HbA1c comparison produced a test statistic of t = 77.774, with a p-value of 3.019×10^{-315} and a Cohen's d effect size of 3.175, indicating a very great and statistically significant improvement. In addition, the Wilcoxon signed-rank test for HbA1c comparison yielded a p-value of 8.706×10^{-100}, further confirming the significance of the observed correspondence between predicted risk

Manuscript received 9 February 2026; Revised 10 March 2026; Accepted 25 March 2026; Available online 30 March 2026
Digital Object Identifier (**DOI**): https://doi.org/10.35882/jeeemi.v8i2.1541

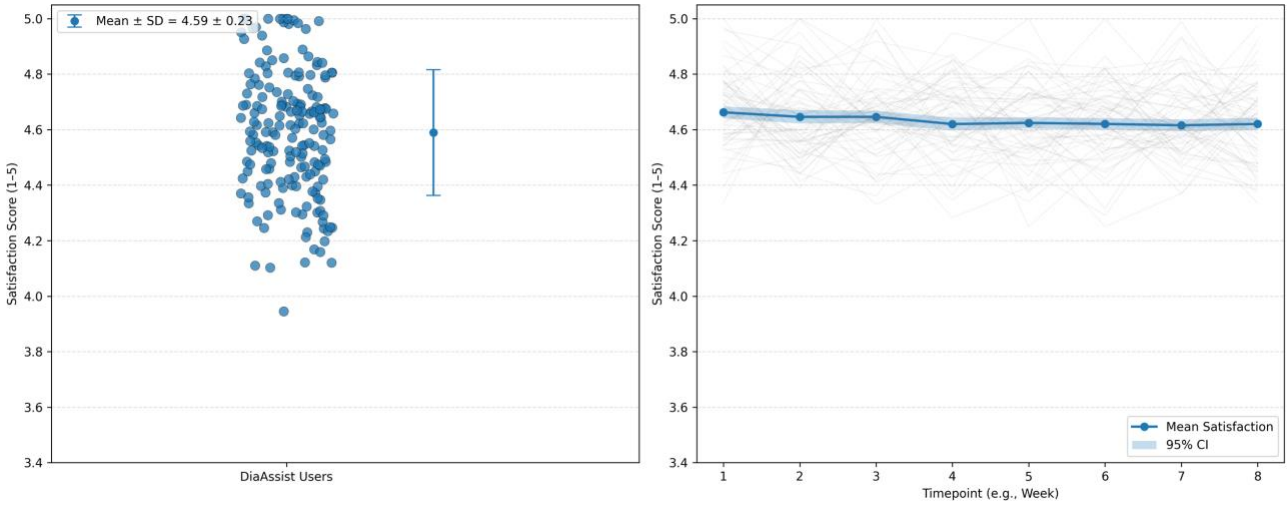

Fig. 4. User satisfaction analysis for the DiaAssist system: (a) distribution of satisfaction scores across users; (b) trend of mean satisfaction levels over monitoring timepoints.

Table 3. Performance Metrics Before and After Optimization

Metric	Before	After	Δ
Accuracy	0.918	**0.997**	0.078
AUC	0.997	**1**	0.003
Brier Score	0.077	**0.045**	-0.032
Cohen's κ	0.805	**0.993**	0.188
MCC	0.821	**0.993**	0.172

scores and HbA1c measurements. Although the p-values are extremely small, this reflects the strong consistent alignment between predicted probabilities and HbA1c measurements across the 625-sample dataset rather than a statistical artifact. The very large effect size (Cohen's d = 3.175) further confirms that the association is not only statistically significant but also clinically meaningful.

Comparative HbA1c distributions before and after prediction optimization are illustrated in Fig. 3(e). and Fig. 3(f)., demonstrating improved correspondence between predicted risk levels and long-term glycemic indicators.

G. Additional Statistical Metrics and Calibration Analysis

Table 3 summarizes the comparative performance of the DiaAssist system before and after model optimization across multiple evaluation metrics.

Calibration performance improved following ensemble optimization. The Brier score decreased from 0.077 to 0.045 (Δ = −0.032), reflecting improved probability accuracy. Concurrently, reliability measures strengthened, with Cohen's κ increasing from 0.805 to 0.993 (Δ = +0.188) and MCC increasing from 0.821 to 0.993 (Δ = +0.172), confirming strong agreement between predicted and reference classifications.

H. Computational Performance and Latency Analysis

The computational efficiency of the DiaAssist system was evaluated to assess its suitability for real-time deployment. Sensor acquisition required approximately 1 second per physiological sampling cycle, reflecting the physical measurement interval rather than processing delay.

Edge-level preprocessing operations, including signal smoothing, normalization, window-based feature extraction, and drift correction, required approximately 12 ms per participant record on the ESP32 dual-core 240 MHz microcontroller. Ensemble inference, including probabilistic aggregation across RF, SVM, and XGBoost classifiers, required approximately 18 ms per record. The total end-to-end computational latency for diabetes risk prediction was therefore approximately 30 ms per record, excluding physiological acquisition time. This latency supports near real-time screening capability. From a computational complexity perspective, inference scales approximately linearly with the number of input samples (O(n)), indicating predictable performance for extended monitoring or larger deployments.

V. Discussion

This section interprets the experimental findings of the DiaAssist system, contextualizes them within related studies, and discusses the limitations and broader

Manuscript received 9 February 2026; Revised 10 March 2026; Accepted 25 March 2026; Available online 30 March 2026
Digital Object Identifier (**DOI**): https://doi.org/10.35882/jeeemi.v8i2.1541

Table 4. Quantitative Comparison with Representative Diabetes Risk Screening Studies

Study	Modality	Accuracy	AUC	Statistical Validation
D. V. K. et al. [11]	Clinical data-based machine learning	0.9	0.94	Accuracy and AUC only
K. Oliullah et al.[12]	Clinical and lifestyle attributes	0.85	0.88	Accuracy-based evaluation
S. Kumari et al. [14]	Ensemble ML using structured clinical data	0.95	0.98	Limited statistical analysis
J. J. Khanam et al. [31]	Clinical dataset (Pima Indians Diabetes Dataset)	0.92	0.96	Limited validation
Proposed (DiaAssist)	Multi-modal IoT biosensing + Ensemble learning	0.997	1	Agreement + Calibration + Significance testing

implications of the proposed non-invasive diabetes risk screening framework. The optimized ensemble model achieved an accuracy of 0.997 and an AUC of 1.000, indicating that it can distinguish between diabetes risk categories with very high discriminative power. The improvement in predicted diabetes risk probabilities after optimization was statistically significant according to the paired t-test ($t = 33.706$, $p = 1.849 \times 10^{-140}$), with a large effect size (Cohen's $d = 1.376$), indicating a strong improvement in prediction separation after model optimization. Classification reliability also improved significantly. McNemar's test produced $\chi^2 = 45.02$ with $p < 0.001$, indicating that the optimized model significantly reduced misclassification errors. Agreement-based evaluation further confirmed this improvement, with Cohen's $\kappa = 0.993$ and Matthews Correlation Coefficient (MCC) = 0.993, demonstrating near-perfect agreement between predicted labels and reference risk categories. The improvement in probability distributions was also confirmed using a Wilcoxon signed-rank test ($p = 5.978 \times 10^{-100}$), indicating that the change in predicted risk probabilities after optimization is statistically significant even without assuming normal distribution of the data (Fig. 4). The physiological relevance of the predicted risk probabilities was evaluated using HbA1c measurements as an external biochemical reference. Pearson correlation analysis yielded a strong positive correlation ($r = 0.91$, $p < 0.001$), indicating that higher predicted diabetes risk probabilities are associated with higher HbA1c values. Agreement between predicted risk classes and HbA1c clinical categories yielded Cohen's $\kappa = 0.92$, indicating substantial to near-perfect categorical alignment. Additional statistical comparison between predicted risk scores and HbA1c values produced $t = 77.774$ ($p = 3.019 \times 10^{-315}$, Cohen's $d = 3.175$) and a Wilcoxon p-value of 8.706×10^{-100}, confirming strong statistical correspondence between non-invasive predictions and biochemical measurements. Furthermore, the Brier score decreased from 0.077 to 0.045, indicating improved probabilistic calibration and more accurate risk probability estimation after ensemble optimization.

Prior studies on diabetes risk prediction typically rely on either structured clinical laboratory variables or single-modality physiological sensing combined with conventional machine learning models. While several of these approaches report strong classification accuracy under controlled conditions, many lack probabilistic calibration assessment, agreement analysis, or validation across multi-modal physiological inputs. To provide an empirical comparison, Table 4 summarizes representative studies discussed in Section II alongside the proposed DiaAssist framework. Reported accuracies in prior works generally range between 0.92 and 0.95, with AUC values between 0.96 and 0.98. In contrast, the optimized DiaAssist ensemble achieved an accuracy of 0.997 and an AUC of 1.000 on the held-out test dataset.

Beyond classification accuracy, the key distinction of the proposed system lies in its comprehensive validation framework. While many prior studies report accuracy or AUC alone, the present work incorporates agreement measures (Cohen's $\kappa = 0.993$; MCC = 0.993), calibration analysis (Brier score = 0.045), and statistical hypothesis testing (paired t-test, Wilcoxon, McNemar's test). This expanded evaluation provides stronger evidence of model reliability and probabilistic stability, which are essential for population-level risk screening. Furthermore, unlike wearable monitoring systems focused primarily on descriptive visualization or trend tracking, DiaAssist integrates multi-modal sensing, edge-level preprocessing, probabilistic ensemble inference, and statistical validation into a unified end-to-end screening architecture. This integration enhances robustness, interpretability, and deployment readiness for preventive healthcare applications.

Several studies have explored machine learning techniques for diabetes risk prediction using clinical datasets. D. V. K. et al. [11] employed machine learning on clinical and demographic data, achieving an

Manuscript received 9 February 2026; Revised 10 March 2026; Accepted 25 March 2026; Available online 30 March 2026
Digital Object Identifier (**DOI**): https://doi.org/10.35882/jeeemi.v8i2.1541

accuracy of 0.90 and an AUC of 0.94; however, their evaluation was limited to conventional metrics without comprehensive statistical validation. K. Oliullah et al. [12] focused on clinical and lifestyle attributes, obtaining an accuracy of 0.85 and an AUC of 0.88, reflecting moderate predictive performance. More recently, S. Kumari et al. [14] applied ensemble machine learning techniques to structured clinical data, achieving superior results with an accuracy of 0.95 and an AUC of 0.98, thereby demonstrating the effectiveness of ensemble approaches over individual models. Finally, J. J. Khanam et al. [31] utilized the Pima Indians Diabetes Dataset and reported an accuracy of 0.92 and an AUC of 0.96, although their validation framework remained limited. In contrast, the proposed DiaAssist system integrates multi-modal IoT-based biosensing with ensemble learning, achieving 0.997 accuracy and an AUC of 1.000, while also incorporating comprehensive statistical validation including agreement analysis, calibration evaluation, and statistical significance testing. This comparison suggests that combining multi-modal physiological sensing with statistically validated ensemble learning can enhance predictive reliability and screening robustness compared with traditional clinical-data-based machine learning approaches.

Despite the encouraging findings, several limitations should be acknowledged. First, the experimental evaluation was conducted using data collected in a controlled, single-center setting. Although stratified sampling and held-out testing were employed, the demographic and metabolic characteristics of the study cohort may not fully reflect those of broader populations. Variations in ethnicity, genetic predisposition, lifestyle behavior, and baseline metabolic profiles across different regions may influence generalizability. Second, while multiple physiological modalities were incorporated, overall system performance remains dependent on sensor stability and signal quality. Long-term sensor drift, device placement variability, environmental noise, and user adherence factors in uncontrolled real-world settings may introduce variability not fully captured during controlled data collection. Third, breath acetone sensing, although physiologically relevant to altered glucose metabolism, may be influenced by external and behavioral factors. Environmental volatile organic compound (VOC) interference and ambient air composition may affect gas sensor readings. Furthermore, dietary patterns such as ketogenic or low-carbohydrate diets can elevate breath acetone levels independently of diabetic risk, potentially introducing classification confounding. Fourth, metabolic baselines and cardiovascular parameters may differ between urban and rural populations due to variations in physical activity patterns, environmental exposures, nutritional habits, and access to healthcare. These contextual factors were not explicitly stratified in the present study. Finally, the proposed framework is designed as a risk screening and decision-support system rather than a standalone diagnostic tool. It should not be interpreted as a replacement for clinical diagnosis or laboratory-based biochemical assessment [37], [38], [39], [40]. Addressing these limitations will require validation on independent multi-center datasets, longitudinal monitoring to assess temporal stability, demographic stratification analysis, and evaluation under real-world deployment conditions.

The findings of this study have important implications for non-invasive and scalable diabetes risk screening systems. The results demonstrate that integrating IoT-based biosensing with ensemble machine learning and comprehensive statistical validation can produce reliable risk estimates suitable for population-level screening. Prior research has shown that IoT-enabled healthcare platforms enable continuous physiological monitoring and remote medical support, particularly in resource-limited settings [8], [9], [10]. In addition, ensemble machine learning approaches have been widely reported to improve predictive performance and model stability in diabetes risk prediction tasks involving heterogeneous datasets [11], [12], [14]. The inclusion of agreement metrics and calibration analysis further strengthens the reliability and interpretability of AI-based medical screening systems [16], [17], [35]. The high user acceptance observed in this study suggests that wearable, non-invasive biosensing platforms can be integrated into remote health-monitoring and preventive healthcare workflows[41], [42], [43], [44], [45]. More broadly, the proposed DiaAssist framework demonstrates how multi-modal physiological sensing, edge computing, and machine-learning analytics can be combined to enable continuous metabolic risk assessment. Recent studies highlight the increasing role of AI-enabled IoT healthcare systems in enabling early detection and monitoring of chronic diseases such as diabetes and cardiovascular disorders [8], [10], [26]. By enabling non-invasive physiological monitoring and data-driven risk inference, such systems may support the transition from traditional episodic diagnostic testing toward continuous preventive health assessment.

VI. Conclusion

The aim of this study was to design and statistically evaluate an AI-enabled IoT-based non-invasive biosensing system for diabetes risk screening, focusing on system architecture, multi-modal data fusion, and engineering-level validation rather than clinical diagnosis. The proposed DiaAssist framework integrates wearable physiological sensing, edge-level preprocessing, ensemble machine learning, and

Manuscript received 9 February 2026; Revised 10 March 2026; Accepted 25 March 2026; Available online 30 March 2026
Digital Object Identifier (**DOI**): https://doi.org/10.35882/jeeemi.v8i2.1541

comprehensive statistical evaluation. Experimental results demonstrate substantial performance improvement after optimization, with accuracy increasing from 0.918 to 0.997, AUC improving from 0.997 to 1.000, Cohen's κ increasing from 0.805 to 0.993, and MCC improving from 0.821 to 0.993, indicating strong classification reliability. Probabilistic calibration also improved, as the Brier score decreased from 0.077 to 0.045, indicating more accurate risk probability estimates. Statistical tests, including the paired t-test, Wilcoxon signed-rank test, and McNemar's test, confirmed that these improvements are statistically significant. Additionally, consistent user satisfaction and stable operation of the IoT sensing platform indicate practical feasibility for repeated non-invasive monitoring. Overall, the results suggest that integrating IoT-based biosensing with ensemble learning and rigorous statistical validation provides an effective and scalable engineering approach for diabetes risk screening and preventive health monitoring. Future work will include multi-center validation across diverse populations, longitudinal monitoring of biomarker stability, integration with an mHealth application for real-time risk tracking, and alignment with medical device regulatory standards. These efforts aim to transition the DiaAssist system from a research prototype to a scalable, real-world preventive healthcare deployment.

Acknowledgment

The authors wish to acknowledge the academic and technical support provided by Terna Engineering College, Navi Mumbai, India. Special thanks are due to the faculty and research scholars for their valuable insights and suggestions during the research process.

Funding

This research received no specific grant from any funding agency in the public, commercial, or not-for-profit sectors.

Data Availability

The data supporting the findings of this study were collected for academic and research purposes and contain sensitive physiological information. For privacy and ethical reasons, the datasets are not publicly available. However, anonymized data and additional methodological details may be made available from the corresponding author upon reasonable request for academic use.

Author Contribution

Prachi Kamble contributed to the conceptualization, system design, data acquisition, methodology development, statistical analysis, and manuscript preparation. Lakshmappa Ragha provided supervision, methodological validation, and a critical review of the manuscript. Prachi Kamble and Yogesh Pingle contributed to the implementation of machine learning, data processing, result analysis, and manuscript revision. All authors reviewed and approved the final version of the manuscript and agreed to be responsible for all aspects of the work, ensuring integrity and accuracy.

Declarations

Ethical Approval

The study was conducted in accordance with institutional research guidelines and approved by the Institutional Ethics Committee of Terna Engineering College. All participants provided written informed consent prior to data collection. The study involved non-invasive physiological measurements for engineering evaluation purposes only, and no therapeutic intervention or clinical treatment was administered. All collected data were anonymized to ensure participant confidentiality.

Consent for Publication Participants.

Consent for publication was given by all participants

Competing Interests

The authors declare no competing interests.

References

[1] G. A. Roth *et al.*, "Global Burden of Cardiovascular Diseases and Risk Factors, 1990–2019," *J. Am. Coll. Cardiol.*, vol. 76, no. 25, pp. 2982–3021, Dec. 2020, doi: 10.1016/j.jacc.2020.11.010.

[2] Md. J. Hossain, Md. Al-Mamun, and Md. R. Islam, "Diabetes mellitus, the fastest growing global public health concern: Early detection should be focused," *Health Sci. Rep.*, vol. 7, no. 3, Mar. 2024, doi: 10.1002/hsr2.2004.

[3] S. Zhang *et al.*, "Wearable non-invasive glucose sensors based on metallic nanomaterials," *Mater. Today Bio*, vol. 20, p. 100638, Jun. 2023, doi: 10.1016/j.mtbio.2023.100638.

[4] U. M. Butt, S. Letchmunan, M. Ali, F. H. Hassan, A. Baqir, and H. H. R. Sherazi, "Machine Learning Based Diabetes Classification and Prediction for Healthcare Applications," *J. Healthc. Eng.*, vol. 2021, pp. 1–17, Sep. 2021, doi: 10.1155/2021/9930985.

[5] M. R. Jadhav, P. R. Wankhede, S. Srivastava, H. N. Bhargaw, and S. Singh, "Breath-based biosensors and system development for noninvasive detection of diabetes: A review," *Diabetes & Metabolic Syndrome: Clinical Research & Reviews*, vol. 18, no. 1, p. 102931, Jan. 2024, doi: 10.1016/j.dsx.2023.102931.

Manuscript received 9 February 2026; Revised 10 March 2026; Accepted 25 March 2026; Available online 30 March 2026
Digital Object Identifier (**DOI**): https://doi.org/10.35882/jeeemi.v8i2.1541

[6] S. Checker, A. B. Yadav, G. V. Sivnath Reddy, and R. Checker, "Advances in Volatile Organic Compounds-Based Biomarker Detection Using Nanomaterial-Integrated Sensor Platforms for Cancer Diagnosis," *ACS Appl. Electron. Mater.*, Mar. 2026, doi: 10.1021/acsaelm.5c02148.

[7] R. Kapur *et al.*, "GlucoBreath: An IoT, ML, and Breath-Based Non-Invasive Glucose Meter," *IEEE Access*, vol. 12, pp. 59346–59360, 2024, doi: 10.1109/ACCESS.2024.3392015.

[8] Muthupandi G, Vikram R, and P. Vidhya Lakshmi, "IoT Wearables for Continuous Health Monitoring," in *Artificial intelligence and IoT in Predictive Healthcare*, Deep Science Publishing, 2025. doi: 10.70593/978-93-7185-397-2_2.

[9] C. A. Patil, A. S. Parab, A. S. Tawade, Y. Pingle, and S. Raul, "IoT based Counter System for Press Fit Machines," in *2024 11th International Conference on Computing for Sustainable Global Development (INDIACom)*, IEEE, Feb. 2024, pp. 64–69. doi: 10.23919/INDIACom61295.2024.10498630.

[10] D. Verma *et al.*, "Internet of things (IoT) in nano-integrated wearable biosensor devices for healthcare applications," *Biosens. Bioelectron. X*, vol. 11, p. 100153, Sep. 2022, doi: 10.1016/j.biosx.2022.100153.

[11] D. V. K. and T. K. Ramesh, "Optimized stacking ensemble models for the prediction of diabetic progression," *Multimed. Tools Appl.*, vol. 82, no. 27, pp. 42901–42925, Nov. 2023, doi: 10.1007/s11042-023-14858-4.

[12] K. Oliullah, M. H. Rasel, Md. M. Islam, Md. R. Islam, Md. A. H. Wadud, and Md. Whaiduzzaman, "A stacked ensemble machine learning approach for the prediction of diabetes," *J. Diabetes Metab. Disord.*, vol. 23, no. 1, pp. 603–617, Nov. 2023, doi: 10.1007/s40200-023-01321-2.

[13] B. Amma N.G., "En-RfRsK: An ensemble machine learning technique for prognostication of diabetes mellitus," *Egyptian Informatics Journal*, vol. 25, p. 100441, Mar. 2024, doi: 10.1016/j.eij.2024.100441.

[14] S. Kumari, D. Kumar, and M. Mittal, "An ensemble approach for classification and prediction of diabetes mellitus using soft voting classifier," *International Journal of Cognitive Computing in Engineering*, vol. 2, pp. 40–46, Jun. 2021, doi: 10.1016/j.ijcce.2021.01.001.

[15] H. Habehh and S. Gohel, "Machine Learning in Healthcare," *Curr. Genomics*, vol. 22, no. 4, pp. 291–300, Dec. 2021, doi: 10.2174/1389202922666210705124359.

[16] M. Scholz and T. Wimmer, "A comparison of classification methods across different data complexity scenarios and datasets," *Expert Syst. Appl.*, vol. 168, p. 114217, Apr. 2021, doi: 10.1016/j.eswa.2020.114217.

[17] K. Denecke, R. May, and O. Rivera-Romero, "Transformer Models in Healthcare: A Survey and Thematic Analysis of Potentials, Shortcomings and Risks," *J. Med. Syst.*, vol. 48, no. 1, p. 23, Feb. 2024, doi: 10.1007/s10916-024-02043-5.

[18] N. A. ElSayed *et al.*, "2. Classification and Diagnosis of Diabetes: Standards of Care in Diabetes—2023," *Diabetes Care*, vol. 46, no. Supplement_1, pp. S19–S40, Jan. 2023, doi: 10.2337/dc23-S002.

[19] Y. Liu and B. Wang, "Advanced applications in chronic disease monitoring using IoT mobile sensing device data, machine learning algorithms and frame theory: a systematic review," *Front. Public Health*, vol. 13, Feb. 2025, doi: 10.3389/fpubh.2025.1510456.

[20] V. Nguyen, P. Ara, D. Simmons, and U. L. Osuagwu, "The Role of Digital Health Technology Interventions in the Prevention of Type 2 Diabetes Mellitus: A Systematic Review," *Clin. Med. Insights Endocrinol. Diabetes*, vol. 17, Jan. 2024, doi: 10.1177/11795514241246419.

[21] C. J. Kelly, A. Karthikesalingam, M. Suleyman, G. Corrado, and D. King, "Key challenges for delivering clinical impact with artificial intelligence," *BMC Med.*, vol. 17, no. 1, p. 195, Dec. 2019, doi: 10.1186/s12916-019-1426-2.

[22] J. S. Varghese, E. N. Peterson, M. K. Ali, and N. Tandon, "Advancing diabetes surveillance ecosystems: a case study of India," *Lancet Diabetes Endocrinol.*, vol. 12, no. 7, pp. 493–502, Jul. 2024, doi: 10.1016/S2213-8587(24)00124-4.

[23] Y. Muramatsu, S. Watanabe, M. Osada, K. Tajima, A. Karashima, and Y. Y. Maruo, "Small Acetone Sensor with a Porous Colorimetric Chip for Breath Acetone Detection Using the Flow–Stop Method," *Chemosensors*, vol. 13, no. 4, p. 136, Apr. 2025, doi: 10.3390/chemosensors13040136.

[24] A. Thati, A. Biswas, S. R. Chowdhury, and T. K. Sau, "Breath Acetone-Based Non-Invasive Detection of Blood Glucose Levels," *International Journal on Smart Sensing and Intelligent Systems*, vol. 8, no. 2, pp. 1244–1260, Jan. 2015, doi: 10.21307/ijssis-2017-805.

[25] Z. Zhou *et al.*, "Digital Health Platform for Improving the Effect of the Active Health Management of Chronic Diseases in the Community: Mixed Methods Exploratory Study," *J. Med. Internet Res.*, vol. 26, p. e50959, Nov. 2024, doi: 10.2196/50959.

[26] K. Fan and Y. Zhao, "Mobile health technology: a novel tool in chronic disease management," *Intelligent Medicine*, vol. 2, no. 1, pp. 41–47, Feb. 2022, doi: 10.1016/j.imed.2021.06.003.

Manuscript received 9 February 2026; Revised 10 March 2026; Accepted 25 March 2026; Available online 30 March 2026
Digital Object Identifier (**DOI**): https://doi.org/10.35882/jeeemi.v8i2.1541

[27] Y.-T. Chang, Y.-Z. Tu, H.-Y. Chiou, K. Lai, and N. C. Yu, "Real-world Benefits of Diabetes Management App Use and Self-monitoring of Blood Glucose on Glycemic Control: Retrospective Analyses," *JMIR Mhealth Uhealth*, vol. 10, no. 6, p. e31764, Jun. 2022, doi: 10.2196/31764.

[28] Z. Guan *et al.*, "Artificial intelligence in diabetes management: Advancements, opportunities, and challenges," *Cell Rep. Med.*, vol. 4, no. 10, p. 101213, Oct. 2023, doi: 10.1016/j.xcrm.2023.101213.

[29] R. Hirani *et al.*, "Artificial Intelligence and Healthcare: A Journey through History, Present Innovations, and Future Possibilities," ., vol. 14, no. 5, p. 557, Apr. 2024, doi: 10.3390/life14050557.

[30] A. Shrivastava *et al.*, "Leveraging XGBoost for Predictive Analytics in Healthcare: Enhancing Disease Diagnosis," in *2024 7th International Conference on Contemporary Computing and Informatics (IC3I)*, IEEE, Sep. 2024, pp. 1666–1672. doi: 10.1109/IC3I61595.2024.10829136.

[31] J. J. Khanam and S. Y. Foo, "A comparison of machine learning algorithms for diabetes prediction," *ICT Express*, vol. 7, no. 4, pp. 432–439, Dec. 2021, doi: 10.1016/j.icte.2021.02.004.

[32] D. Sisodia and D. S. Sisodia, "Prediction of Diabetes using Classification Algorithms," *Procedia Comput. Sci.*, vol. 132, pp. 1578–1585, 2018, doi: 10.1016/j.procs.2018.05.122.

[33] M. Salmi, D. Atif, D. Oliva, A. Abraham, and S. Ventura, "Handling imbalanced medical datasets: review of a decade of research," *Artif. Intell. Rev.*, vol. 57, no. 10, p. 273, Sep. 2024, doi: 10.1007/s10462-024-10884-2.

[34] R. J. Chen, M. Y. Lu, T. Y. Chen, D. F. K. Williamson, and F. Mahmood, "Synthetic data in machine learning for medicine and healthcare," *Nat. Biomed. Eng.*, vol. 5, no. 6, pp. 493–497, Jun. 2021, doi: 10.1038/s41551-021-00751-8.

[35] S. Padhy, S. Dash, S. Routray, S. Ahmad, J. Nazeer, and A. Alam, "IoT-Based Hybrid Ensemble Machine Learning Model for Efficient Diabetes Mellitus Prediction," *Comput. Intell. Neurosci.*, vol. 2022, pp. 1–11, May 2022, doi: 10.1155/2022/2389636.

[36] Y. Ghazizadeh, "Machine learning-based diabetes prediction: A comprehensive study on predictive modeling and risk assessment," *Journal of Clinical Images and Medical Case Reports*, vol. 6, no. 5, May 2025, doi: 10.52768/2766-7820/3578.

[37] Y. A. Fahim, I. W. Hasani, S. Kabba, and W. M. Ragab, "Artificial intelligence in healthcare and medicine: clinical applications, therapeutic advances, and future perspectives," *Eur. J. Med. Res.*, vol. 30, no. 1, p. 848, Sep. 2025, doi: 10.1186/s40001-025-03196-w.

[38] B. Chen, Y. Wang, X. Xie, B. Fan, W. Zhang, and G. Sun, "Trends in AI-based diagnosis and intervention of metabolic diseases: a bibliometric analysis of the literature from 2000 to 2024," *Front. Med. (Lausanne).*, vol. 12, Dec. 2025, doi: 10.3389/fmed.2025.1698366.

[39] A. I. Stoumpos, F. Kitsios, and M. A. Talias, "Digital Transformation in Healthcare: Technology Acceptance and Its Applications," *Int. J. Environ. Res. Public Health*, vol. 20, no. 4, p. 3407, Feb. 2023, doi: 10.3390/ijerph20043407.

[40] Y. P. Pingle and L. K. Ragha, "Statistical assessment of Indian classical music's role in diabetes, thyroid, hypertension management," *International Journal of Information Technology*, vol. 17, no. 1, pp. 423–429, Jan. 2025, doi: 10.1007/s41870-024-02227-9.

[41] E. Maimaitijiang, M. Aihaiti, and Y. Mamatjan, "An Explainable AI Framework for Online Diabetes Risk Prediction with a Personalized Chatbot Assistant," *Electronics (Basel).*, vol. 14, no. 18, p. 3738, Sep. 2025, doi: 10.3390/electronics14183738.

[42] A. F. Scheideman *et al.*, "Machine Learning to Diagnose Complications of Diabetes," *J. Diabetes Sci. Technol.*, vol. 19, no. 6, pp. 1650–1670, Nov. 2025, doi: 10.1177/19322968251365245.

[43] T. Liu *et al.*, "Emerging Wearable Acoustic Sensing Technologies," *Advanced Science*, vol. 12, no. 6, Feb. 2025, doi: 10.1002/advs.202408653.

[44] Y.-T. Chang, Y.-Z. Tu, H.-Y. Chiou, K. Lai, and N. C. Yu, "Real-world Benefits of Diabetes Management App Use and Self-monitoring of Blood Glucose on Glycemic Control: Retrospective Analyses," *JMIR Mhealth Uhealth*, vol. 10, no. 6, p. e31764, Jun. 2022, doi: 10.2196/31764.

[45] Z. Guan *et al.*, "Artificial intelligence in diabetes management: Advancements, opportunities, and challenges," *Cell Rep. Med.*, vol. 4, no. 10, p. 101213, Oct. 2023, doi: 10.1016/j.xcrm.2023.101213.

[46] I. Kavakiotis, O. Tsave, A. Salifoglou, N. Maglaveras, I. Vlahavas, and I. Chouvarda, "Machine Learning and Data Mining Methods in Diabetes Research," *Comput. Struct. Biotechnol. J.*, vol. 15, pp. 104–116, 2017, doi: 10.1016/j.csbj.2016.12.005.

Author Biography

Prachi C. Kamble received the Master's degree in Electronics and Telecommunication Engineering from

Manuscript received 9 February 2026; Revised 10 March 2026; Accepted 25 March 2026; Available online 30 March 2026
Digital Object Identifier (**DOI**): https://doi.org/10.35882/jeeemi.v8i2.1541

Terna Engineering College, Navi Mumbai, India, affiliated with the University of Mumbai, in 2013. She is currently pursuing the Ph.D. degree at Terna Engineering College, University of Mumbai. She has more than 15 years of academic experience in engineering education and has been actively involved in teaching, research, and academic mentoring. Her research interests include the Internet of Things (IoT), wireless communication systems, embedded systems, and machine learning applications in healthcare technologies. She has contributed to these areas through academic research publications and professional development activities. Her current research focuses on AI-enabled IoT-based healthcare systems and non-invasive biosensing technologies for early disease detection.

Lakshmappa K. Ragha received the M.E. degree in Digital Electronics Engineering from Karnataka University, Dharwad, India, in 1997, and the Ph.D. degree in Electronics Engineering from the University of Mumbai, India. He served as Professor in the Department of Electronics and Telecommunication Engineering and as Ex-Principal of Terna Engineering College, Navi Mumbai, India. His research contributions include microwave bioeffects, numerical simulation of radiating systems, and signal processing techniques. His academic interests also include speech processing, noise reduction methods, and applications of the Internet of Things (IoT). He has supervised numerous postgraduate and doctoral research scholars and has published more than 50 research papers in peer-reviewed journals and international conferences. He is also an active member of several professional societies.

Yogesh Pingle received the Ph.D. degree in Computer Engineering from the University of Mumbai, India, along with the M.E. and B.E. degrees in Computer Engineering. He is currently working as Deputy Head of Department and Assistant Professor in the Department of Computer Science and Engineering (Data Science) at Vidyavardhini's College of Engineering and Technology, Vasai, Maharashtra, India. He has published more than 40 research papers in Scopus-indexed journals and IEEE publications and has presented his work at several national and international conferences. His research interests include machine learning, Internet of Things (IoT), data-driven intelligent systems, and applications of artificial intelligence in healthcare and music therapy.

Manuscript received 9 February 2026; Revised 10 March 2026; Accepted 25 March 2026; Available online 30 March 2026
Digital Object Identifier (**DOI**): https://doi.org/10.35882/jeeemi.v8i2.1541

Journal of Electronics, Electromedical Engineering, and Medical Informatics
Homepage: jeeemi.org; Vol. 8, No. 2, April 2026, pp: 517-536 e-ISSN: 2656-8632

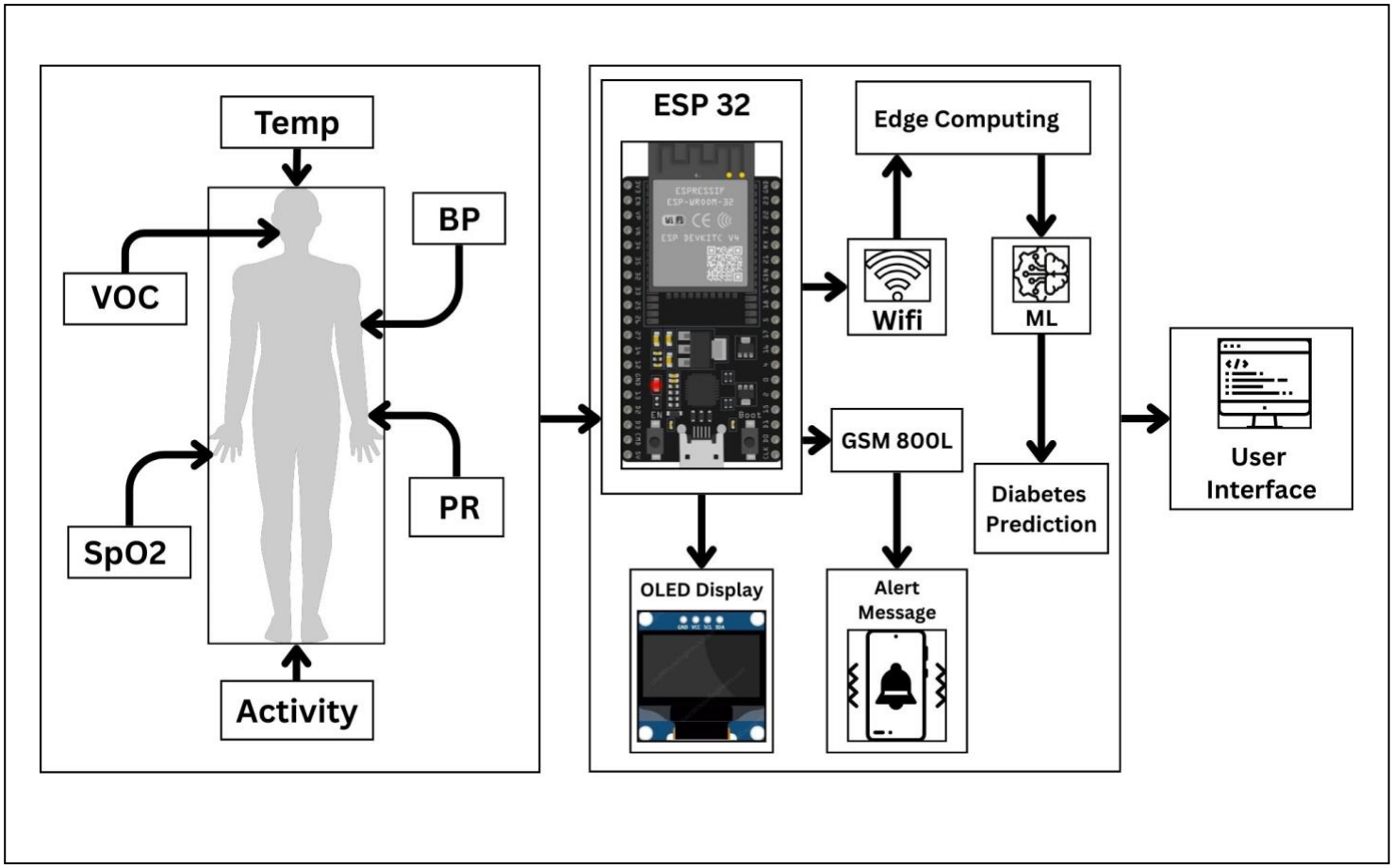

Manuscript received 9 February 2026; Revised 10 March 2026; Accepted 25 March 2026; Available online 30 March 2026
Digital Object Identifier (**DOI**): https://doi.org/10.35882/jeeemi.v8i2.1541